Antiflow of mesons in the high baryon density region

Zuo-Wen Liu and Shusu Shi [*]

*Key Laboratory of Quark and Lepton Physics (MOE) and Institute of Particle Physics,
Central China Normal University, Wuhan 430079, China*

The E895 and STAR experiments demonstrate that the slopes of directed flow with respect to rapidity $(dv_1/dy|_{y=0})$ of mesons are negative in the low transverse momentum (p_T) region, $p_T < 0.8$ GeV/c, in Au + Au collisions at $\sqrt{s_{NN}} = 3.0$–3.9 GeV. Using the transport model JAM, we investigate the directed flow of $\pi^{\pm}$, $K^{\pm}$, and K^0 as functions of rapidity, p_T, and collision energy in Au + Au collisions at the same energies as those in the E895 and STAR experiments. We find that the JAM model can qualitatively reproduce the antiflow of K_S^0 observed in the E895 experiment. The v_1 slopes of pions and kaons are analyzed as functions of the p_T window, revealing a strong p_T dependence of the v_1 slopes. Negative v_1 slopes are observed in the low p_T region, $p_T < 0.8$ GeV/c, while positive slopes are shown in the higher p_T region. We find that the shadowing effect from spectators is crucial in generating the antiflow of mesons at low p_T in the high baryon density region.

I. INTRODUCTION

The collective flow (v_n) is the event anisotropy of final state particles in heavy-ion collisions, which can be defined by Fourier expansion of the particle distribution with respected to the reaction plane [1,2]:

$$E\frac{d^3N}{d^3p} = \frac{1}{2\pi}\frac{d^2N}{p_T\,dp_T\,dy}\left(1 + \sum_{n=1}^{\infty} 2v_n \cos\left[n(\phi - \Psi_r)\right]\right),\tag{1}$$

where ϕ, Ψ_r, and v_n represent the azimuth of final state particle in the laboratory frame, the azimuth of the reaction plane, and the nth harmonic coefficient of the Fourier series, respectively. The collective flow carries the information of the created medium in heavy-ion collisions [3], and is sensitive to the properties and the equation of state (EoS) of the medium. The first-order coefficient, known as directed flow (v_1), signifies the sideward collective motion of particles along the direction of the impact parameter [4]. In the context of heavy-ion collisions, v_1 offers valuable insights into the behavior of quark-gluon plasma (QGP) and its transition to a hadronic phase. It acts as a sensitive probe for examining the properties of strongly interacting matter under extreme conditions in heavy-ion collisions [5–13]. At the same time, it can reveal the interplay between initial compression and tilted expansion [14,15], thereby playing an important role in exploring the quantum chromodynamics (QCD) phase diagram, especially in the high baryon density region with a large baryon chemical potential μ_B [16–27]. Moreover, v_1 measurements impose constraints on the EoS and identify its softest point in the QCD phase diagram [28–36]. Thus, v_1 study in the high baryon density region is pivotal for enhancing our

understanding of the QCD phase diagram and the nature of strongly interacting matter at extreme densities.

The sign of v_1 is commonly used to describe the deflection behavior of particles in heavy-ion collisions. A positive v_1 indicates that more freeze-out particles are emitted in the direction aligned with the spectators, while a negative v_1 indicates that more particles are emitted in the direction opposite to the spectators [37]. In high energy heavy-ion collisions, a negative v_1 at positive rapidity, leading to a negative slope at midrapidity $(dv_1/dy|_{y=0})$, known as antiflow, can be attributed to the tilted expansion prevailing over the initial compression [14,38–40]. On the other hand, at lower collision energies $(\sqrt{s_{NN}} < 10$ GeV), the spectator shadowing effect becomes non-negligible, introducing another factor influencing the flow observable. The shadowing effect generates negative elliptic flow, as observed in experiments such as Au + Au collisions at $\sqrt{s_{NN}} = 3.0$ GeV from the STAR detector at the Relativistic Heavy Ion Collider (RHIC-STAR), where $\mu_B \approx 720$ MeV [41]. Regarding v_1, the antiflow of K_S^0 was observed in Au + Au collisions at $\sqrt{s_{NN}} = 3.83$ GeV by the E895 experiment at the Alternating Gradient Synchrotron (AGS) over two decades ago [42,43]. The kaon antiflow is widely attributed to the repulsive kaon potential in the high baryon density region [43–49]. It is also worth studying whether meson antiflow is possibly caused by the spectator shadowing effect [50].

The passing time of spectators $(\sim 2R/\gamma\beta)$ closely matches the average time of particle freeze-out [50–52], where R is the radius of nuclei, γ is the Lorentz contraction factor, and β is the velocity of the spectators as a fraction of the speed of light. It leads to freeze-out particles being shadowed by the spectators. Table I lists the spectator passing times t_p in the center-of-mass frame for Au + Au collisions at $\sqrt{s_{NN}} = 3.0$, 3.2, 3.5, and 3.9 GeV. The average time of particle freeze-out t_m is estimated using the JET AA

TABLE I. Rapidity y, velocity β, the spectator passing time t_p, the hadron freeze-out mean time t_m in the JAM model, and their ratio t_p/t_m from Au+Au collisions at $\sqrt{s_{NN}} = 3.0$, 3.2, 3.5, and 3.9 GeV. Note that t_m is calculated from all hadrons over $|\eta| < 1$.

$\sqrt{s_{NN}}$ (GeV)	y	β (c)	t_p (fm/c)	t_m (fm/c)	t_p/t_m
3.0	1.06	0.79	11.00	16.99	0.65
3.2	1.13	0.81	10.07	16.68	0.60
3.5	1.25	0.85	8.72	16.34	0.53
3.9	1.37	0.88	7.59	16.01	0.47

Microscopic Transport Model (JAM) [53]. The ratio of t_p to t_m indicates that the spectator passing time is about half of the average time of particle freeze-out in Au + Au collisions at $\sqrt{s_{NN}} = 3.0$–3.9 GeV. Furthermore, this ratio increases as the collision energy decreases, suggesting that the spectator shadowing effect becomes more significant at lower collision energies. Using the JAM model, we investigate the shadowing effect on the v_1 of pions and kaons in Au + Au collisions at $\sqrt{s_{NN}} = 3.0$–3.9 GeV, corresponding to a μ_B coverage from 630 to 720 MeV. We find that antiflow is observed not only for K^0 but also for charged pions and kaons in the low p_T region.

The rest of this paper is organized as follows. We introduce the JAM model in Sec. II. Then, in Sec. III, we present a comparison of K_S^0 antiflow from the E895 experiment to JAM calculations, along with a detailed study of v_1 slopes of pions and kaons with the JAM model at the same collision energies as the STAR experiment [54]. To study the shadowing effect from spectators, we compare the results with and without spectators from JAM model. Finally, we provide a summary in Sec. IV.

II. JAM MODEL

The JAM model is a hadronic transport model capable of simulating the evolution of relativistic heavy-ion collisions [53]. In this model, particle production includes resonance excitation, string production, and their decay contributions, similar to other transport models such as RQMD, AMPT, and PHSD [55–58]. Two different approaches are used to describe the effect of the EoS in JAM. One is the cascade method based on the modified two-body scattering [59], while the other involves the nuclear mean-field method implemented with the relativistic quantum molecular dynamics approach [60].

It has been demonstrated that the baryonic mean-field potential plays a significant role in the high baryon density region. JAM model calculations cooperating with baryonic mean-field have successfully described the v_1 and v_2 of baryons in Au + Au collisions at $\sqrt{s_{NN}} = 3.0$ GeV from RHIC-STAR [41,61]. However, the mean-field mode is not suitable for the v_1 of mesons in the high baryon density region, probably due to the implementation of the strong repulsive baryonic potential [62]. The cascade mode describes the v_1 of pions and kaons better than the baryonic mean-field mode at $\sqrt{s_{NN}} < 4.5$ GeV, as illustrated in Refs. [15,34,41,62–64]. Therefore, we will focus on the JAM model in cascade mode for the following meson v_1 study. Additionally, JAM provides
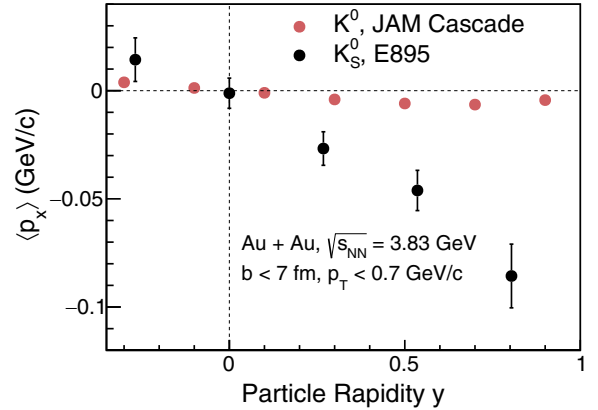

FIG. 1. The directed transverse flow $\langle p_x \rangle$ of K^0 from JAM calculations (red circles), and that of K_S^0 from E895 experiment (black circles) as a function of rapidity in Au + Au collisions at $\sqrt{s_{NN}} = 3.83$ GeV. Note that the normalized rapidity from E895 data has been converted to the center-of-mass frame to enable a direct comparison.

an option to retain or remove spectators during the nuclear matter evolution in heavy-ion collisions. We take advantage of this feature to investigate the nontrivial shadowing effect caused by spectators in the high baryon density region.

In this work, we use version 2.1 of the JAM model to generate Monte Carlo event samples for Au + Au collisions at $\sqrt{s_{NN}} = 3.0$, 3.2, 3.5, and 3.9 GeV. We employ the default cascade mode and the cascade mode without spectators to study the antiflow of mesons in heavy-ion collisions within the high baryon density region. Event centrality is defined by the reference multiplicity, which counts the total number of charged pions, charged kaons, protons, and antiprotons within the pseudorapidity region of $|\eta| < 0.5$, which is same as STAR experimental analysis [54]. The azimuth of the reaction plane is zero in the model, thus the directed flow can be calculated by $v_1 = \langle \cos(\phi) \rangle$. In experiments, as the reaction plane is unknown, the event plane method is used for the v_1 measurements [1]. Using the JAM model, we compare the results from the event plane method, following the STAR experiment [41], to those of $\langle \cos(\phi) \rangle$. The results from the two methods exhibit good consistency in the model. The statistical error is smaller in the case of $\langle \cos(\phi) \rangle$ as it does not require resolution correction due to the event plane estimate. We will present the results of $\langle \cos(\phi) \rangle$ in the following.

III. RESULTS AND DISCUSSIONS

We compare the measurements of directed transverse flow $\langle p_x \rangle$ as a function of rapidity from the E895 experiment with JAM calculations. The experimental measurement of $\langle p_x \rangle$ extracted from Au + Au collisions at $\sqrt{s_{NN}} = 3.83$ GeV by the E895 Collaboration [42,43] is shown as black circles in Fig. 1. To facilitate a direct comparison, the normalized rapidity from E895 data has been converted to the rapidity in the center-of-mass frame [42,43]. The JAM calculations with cascade mode are denoted by red circles, and they are constrained by the same impact parameter range and transverse momentum cut as the data. Note that K^0 in JAM includes both K_S^0 and K_L^0 since the model cannot separate K_S^0 and K_L^0. The model can
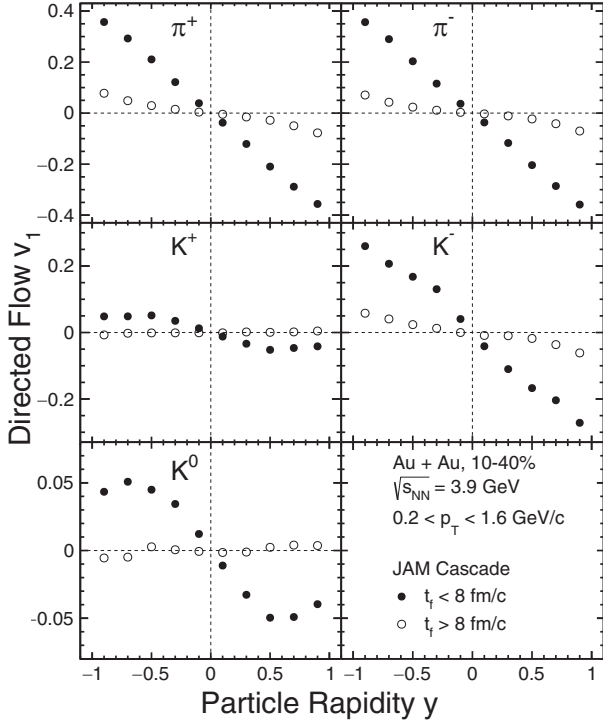
FIG. 2. The directed flow as a function of rapidity in 10–40% most central Au + Au collisions at $\sqrt{s_{NN}} = 3.9$ GeV from the JAM cascade mode, where black solid and open circles denote the particles whose freeze-out times are less and more than 8 fm/c, respectively. The left and right panels depict results of particles (π^+, K^+, and K^0) and the corresponding antiparticles (π^- and K^-), respectively.

reproduce the antiflow of K_S^0 in midrapidity but underestimates the v_1 strength. The discrepancy between the model and the data might be due to the lack of a kaon potential in the JAM cascade mode. Since the model can reproduce the negative v_1 slope of K_S^0 in midrapidity as observed in the experimental data, we will further investigate the impact of the shadowing effect with the JAM model, which is important for the meson v_1 in the high baryon density region.

First, we explore the time evolution of directed flow. As shown in Table I, the spectator passing time is about 8 fm/c in Au + Au collisions at $\sqrt{s_{NN}} = 3.9$ GeV. It is anticipated that particles with a freeze-out time of less than 8 fm/c would be shadowed by the passing spectators, potentially influencing the development of directed flow. Figure 2 depicts the freeze-out time dependence of $v_1(y)$ for pions (π^+ and π^-) and kaons (K^+, K^-, and K^0) in the 10–40% most central Au + Au collisions at $\sqrt{s_{NN}} = 3.9$ GeV from JAM calculations. The solid circles represent the particles that freeze out prior to the passage of the spectator, and the open circles represent those that freeze out after the spectator has passed. Distinct negative v_1 slopes around midrapidity are observed for pions and kaons with a freeze-out time of less than 8 fm/c, and the v_1 slopes approach zero for pions and kaons with freeze-out times exceeding 8 fm/c. This implies that particles freezing out earlier experience a significant shadowing effect from spectators, leading to the observed antiflow. As time progresses and the shadowing effect weakens, the v_1 slopes approach zero for particles with later freeze-out times.
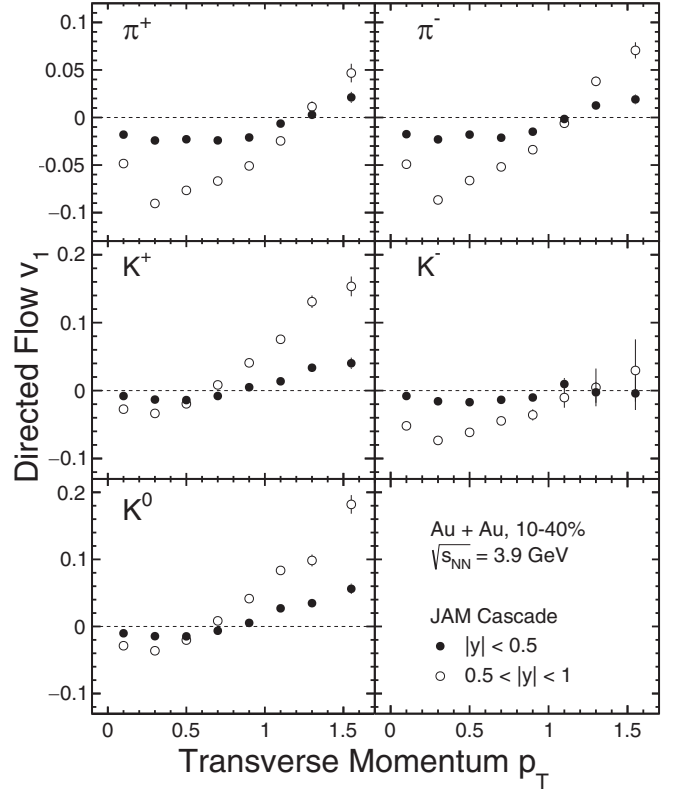

FIG. 3. The directed flow as a function of p_T in 10–40% most central Au + Au collisions at $\sqrt{s_{NN}} = 3.9$ GeV from the JAM cascade mode, where black solid circles are for particles in midrapidity ($|y| < 0.5$) and open circles are for forward rapidity ($0.5 < |y| < 1$). The left and right panels depict results of particles (π^+, K^+, and K^0) and the corresponding antiparticles (π^- and K^-), respectively.

In addition to the spectator shadowing effect being evident in the time evolution, it is expected that particles in the forward rapidity region exhibit greater sensitivity to the shadowing effect compared to those in the midrapidity region, as the former are in closer proximity to the spectator [31,64]. Note that the spectator rapidity is 1.37 at $\sqrt{s_{NN}} = 3.9$ GeV, as shown in Table I. Figure 3 illustrates the transverse momentum dependence of v_1 from midrapidity (solid circles) and forward rapidity (open circles) in 10–40% most central Au + Au collisions at $\sqrt{s_{NN}} = 3.9$ GeV, obtained from JAM calculations. There is a clear negative v_1 at low p_T for pions (π^+ and π^-) and kaons (K^+, K^-, and K^0) at midrapidity ($|y| < 0.5$). The value of v_1 in the forward rapidity region ($0.5 < |y| < 1$), close to the spectator rapidity, shows more negativity. This indicates that a well-defined antiflow is formed at low p_T. Furthermore, The v_1 values for pions exhibit more negativity at low p_T compared to those for kaons, which could be attributed to the significantly larger scattering cross-section of pions relative to kaons ($\sigma_{K_0+p} \approx 10$ mb and $\sigma_{\pi+p} \approx 100$ mb) [43].

The time evolution and p_T dependence of v_1 suggest a negative contribution to v_1 of mesons arising from the spectator shadowing effect. Further study is carried out by removing the spectators in the JAM model. We investigate the v_1 of pions and kaons in an overall transverse momentum (p_T)
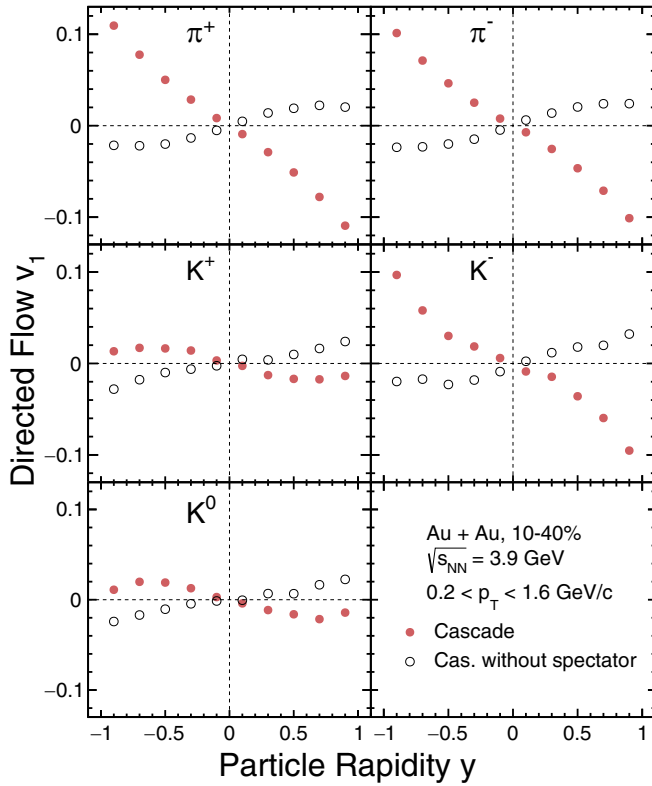
FIG. 4. The directed flow as a function of rapidity in 10–40% most central Au + Au collisions at $\sqrt{s_{NN}}$ = 3.9 GeV from JAM in default cascade mode (red solid circles) and in cascade mode without spectator (open circles). The left and right panels depict results of particles (π^+, K^+, and K^0) and the corresponding antiparticles (π^- and K^-), respectively.

FIG. 5. The directed flow as a function of rapidity in different p_T windows for π^+ (left panels) and K^0 (right panels) in 10–40% most central Au + Au collisions at $\sqrt{s_{NN}}$ = 3.9 GeV from JAM cascade mode (red solid circles) and cascade mode without spectator (open circles).

window ($0.2 < p_T < 1.6$ GeV/c), which is the same as the acceptance range of the STAR experiment [54]. In Fig. 4, the rapidity dependence of directed flow for particles (π^+, K^+, and K^0) and their corresponding anti-particles (π^- and K^-) in 10–40% Au + Au collisions at $\sqrt{s_{NN}}$ = 3.9 GeV is shown for JAM calculations in default cascade mode and cascade mode without spectators. It is observed that JAM in cascade mode predicts negative midrapidity v_1 slopes for pions and kaons. On the other hand, JAM in cascade mode without spectators shows positive v_1 slopes, in contrast to the one with spectator interactions. This implies that the shadowing effect from spectators leads to antiflow of mesons in heavy-ion collisions in the high baryon density region. We studied $dv_1/dy|_{y=0}$ of pions (π^+ and π^-) and kaons (K^+, K^-, and K^0) in JAM, and found that there is no strong charge dependence for the formation of antiflow. To facilitate the following discussion, we take π^+ and K^0 as examples.

Then, we investigate the v_1 distribution in the narrow transverse momentum windows. The rapidity dependence of π^+ and K^0 v_1 within different p_T windows in 10–40% Au + Au collisions at $\sqrt{s_{NN}}$ = 3.9 GeV is presented in Fig. 5. JAM in cascade mode depicts negative v_1 slopes at midrapidity for π^+ and K^0 v_1 at $p_T < 0.8$ GeV/c. The magnitude of v_1 slopes from the cascade mode without spectators decreases compared to those with spectators in the top two panels of
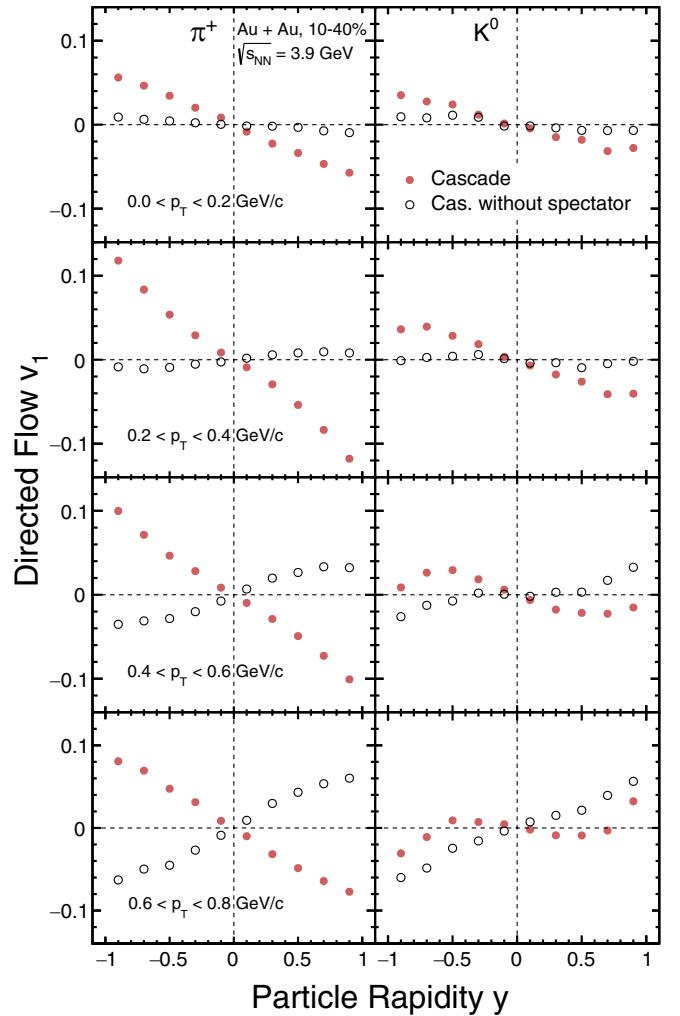
Fig. 5 (with a p_T window of $0 < p_T < 0.2$ GeV/c). As the p_T increases, v_1 slopes of π^+ and K^0 from cascade mode without spectators turn positive rapidly, and clear positive v_1 slopes can be observed when $0.6 < p_T < 0.8$ GeV/c as shown in the bottom two panels of Fig. 5. Meanwhile, the v_1 slopes of π^+ and K^0 from default cascade mode remain negative. The p_T dependence of $v_1(y)$ and the discrepancy between cascade mode with and without spectators indicate that the shadowing effect from spectators is one of the important reasons for the antiflow of π^+ and K^0.

Besides the p_T window, the shadowing effect is also sensitive to the collision centrality. The number of spectator nucleons is larger in more peripheral collisions, thus suggesting that the shadowing effect should be stronger. Figure 6 shows the p_T dependence of v_1 slope at midrapidity for K^0 across three event centralities (0–10%, 10–40%, and 40–60%) in Au + Au collisions at $\sqrt{s_{NN}}$ = 3.9 GeV. It is clearly observed that antiflow for K^0 occurs at low p_T in three
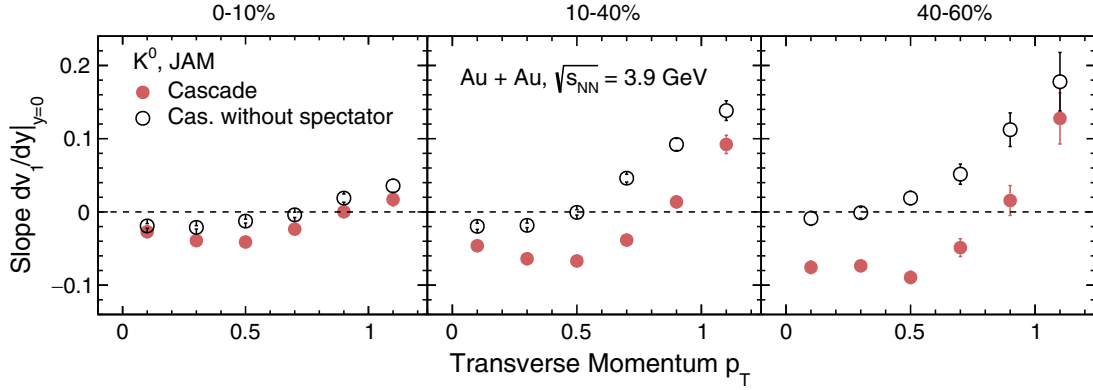
FIG. 6. The v_1 slopes at midrapidity ($dv_1/dy|_{y=0}$) as a function of p_T window for K^0 in 0–10%, 10–40%, and 40–60% most central Au + Au collisions at $\sqrt{s_{NN}} = 3.9$ GeV from the JAM cascade mode (red solid circles) and cascade mode without spectators (open circles). The $dv_1/dy|_{y=0}$ is characterized by the linear term in a fit of the function $v_1(y) = ay + by^3$; the fit range is $-1 < y < 0$.

centralities ($p_T < 0.8$ GeV/c for 0–10%, $p_T < 0.6$ GeV/c for 10–40%, and $p_T < 0.4$ GeV/c for 40–60%) in JAM cascade mode both with and without spectator interactions. JAM with spectators pushes the v_1 slopes of K^0 to be more negative compared to the same model without spectators. Moreover, the magnitude of the v_1 slope in peripheral collisions (40–60%) is greater than that in central collisions (0–10%) in the low p_T region, due to a stronger shadowing effect caused by the increased number of spectators in peripheral collisions. The strong centrality dependence of the v_1 slope confirms that the observed antiflow of K^0 at low p_T could be attributed to the shadowing effect from spectators.

The STAR experiment recently presented preliminary results on identified particle v_1 in Au + Au collisions at $\sqrt{s_{NN}} = 3.0, 3.2, 3.5,$ and 3.9 GeV, where antiflow of mesons was observed at low p_T in these preliminary results [54]. Figure 7 shows v_1 slopes at midrapidity of K^0 as a function of p_T in Au + Au collisions with 10–40% centrality at $\sqrt{s_{NN}} = 3.0, 3.2, 3.5,$ and 3.9 GeV from JAM model calculations. The antiflow of K^0 at low p_T ($p_T < 0.8$ GeV/c) is captured at these four collision energies by JAM in cascade mode. However, for the JAM cascade mode without spectators, the v_1 slopes are closer to zero from negative direction compared to those with spectators. In particular, the antiflow of K^0 cannot be observed at all in the shown p_T range at $\sqrt{s_{NN}} = 3.0$ GeV in JAM without spectators, and the difference in v_1 slope is more evident between JAM with and without spectators. This is probably because the strongest shadowing effect experienced by K^0, characterized by the largest t_p/t_m ratio in Table I among the four collision energies, is not accounted for in JAM without spectators. The comparison between JAM mode with and without spectators implies that the shadowing effect from spectators plays an important role in the kaon antiflow at low p_T in noncentral heavy-ion collisions within the high baryon density region.

IV. SUMMARY

In summary, we present calculations of the directed flow of $\pi^\pm$, $K^\pm$, and K^0 in Au + Au collisions at $\sqrt{s_{NN}} = 3.0, 3.2,$ 3.5, and 3.9 GeV using the hadronic transport model JAM.

The JAM cascade mode can qualitatively reproduce the K_S^0 antiflow observed by the E895 experiment in Au + Au collisions at $\sqrt{s_{NN}} = 3.83$ GeV. Pions and kaons exhibit negative midrapidity v_1 slopes in the low p_T region, $p_T < 0.8$ GeV/c, while the slopes become positive in the higher p_T region. The time evolution of v_1 reveals that the pions and kaons with earlier freeze-out time exhibit distinct negative v_1 slopes around midrapidity, contrasting with a flat v_1 distribution from those with later freeze-out time. And the v_1 values in the forward rapidity are more negative compared to those in the midrapidity. Furthermore, the centrality dependence of the v_1 slope shows that slopes are more negative in more peripheral collisions, which aligns with the expected spectator shadowing effect. To investigate the shadowing effect, we analyze the v_1 slopes of mesons using the JAM model in cascade mode with and
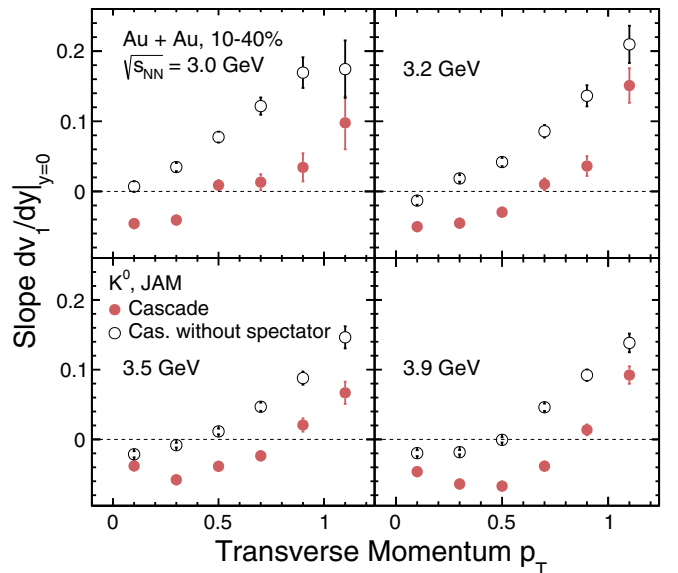

FIG. 7. The v_1 slopes at midrapidity ($dv_1/dy|_{y=0}$) as a function of p_T window for K^0 in 10–40% most central Au + Au collisions at $\sqrt{s_{NN}} = 3.0, 3.2, 3.5,$ and 3.9 GeV form JAM cascade mode (red solid circles) and cascade mode without spectator (open circles).

without spectator. The findings indicate that the shadowing effect from spectators turns positive v_1 slopes into negative ones in the low p_T region at $\sqrt{s_{NN}} = 3.0$–3.9 GeV.

It suggests that in heavy-ion collisions in the high baryon density region, the shadowing effect, arising from the presence of spectators, influences the motion of particles, leading to an antiflow phenomenon of mesons where these particles move opposite to the normal flow direction. The kaon potential, often considered as a significant factor in understanding kaon antiflow, may not be the sole or primary source. The shadowing effect could also contribute significantly. It also implies that the dynamics of high-density nuclear collisions are complex, with multiple factors influencing the collective flow observable. The shadowing effect from spectators plays an important role in understanding the observed phenomena.

[1] A. M. Poskanzer and S. A. Voloshin, Phys. Rev. C **58**, 1671 (1998).

[2] S. A. Voloshin, A. M. Poskanzer, and R. Snellings, in *Relativistic Heavy Ion Physics*, edited by R. Stock, Landolt-Börnstein, Group I, Elementary Particles, Nuclei and Atoms (Springer, Berlin, 2010), Vol. 23, p. 293.

[3] C. M. Hung and E. V. Shuryak, Phys. Rev. Lett. **75**, 4003 (1995).

[4] A. Bilandzic, R. Snellings, and S. Voloshin, Phys. Rev. C **83**, 044913 (2011).

[5] C. Gale, S. Jeon, B. Schenke, P. Tribedy, and R. Venugopalan, Phys. Rev. Lett. **110**, 012302 (2013).

[6] B. Schenke, S. Jeon, and C. Gale, Phys. Rev. Lett. **106**, 042301 (2011).

[7] B. Schenke, S. Jeon, and C. Gale, Phys. Rev. C **82**, 014903 (2010).

[8] S. Ryu, V. Jupic, and C. Shen, Phys. Rev. C **104**, 054908 (2021).

[9] Y. B. Ivanov and A. A. Soldatov, Phys. Rev. C **102**, 024916 (2020).

[10] N. S. Tsegelnik, E. E. Kolomeitsev, and V. Voronyuk, Phys. Rev. C **107**, 034906 (2023).

[11] Z.-F. Jiang, X.-Y. Wu, S. Cao, and B.-W. Zhang, Phys. Rev. C **107**, 034904 (2023).

[12] Z.-F. Jiang, X.-Y. Wu, S. Cao, and B.-W. Zhang, Phys. Rev. C **108**, 064904 (2023).

[13] I. Karpenko and J. Cimerman, EPJ Web Conf. **296**, 04003 (2024).

[14] P. Bożek and I. Wyskiel, Phys. Rev. C **81**, 054902 (2010).

[15] Y. Nara and A. Ohnishi, Phys. Rev. C **105**, 014911 (2022).

[16] A. Bzdak, S. Esumi, V. Koch, J. Liao, M. Stephanov, and N. Xu, Phys. Rep. **853**, 1 (2020).

[17] J. Chen *et al.*, arXiv:2407.02935

[18] X. Luo, S. Shi, N. Xu, and Y. Zhang, Particles **3**, 278 (2020).

[19] Y. B. Ivanov and M. Kozhevnikova, Phys. Rev. C **110**, 014907 (2024).

[20] C. Shen and S. Alzhrani, Phys. Rev. C **102**, 014909 (2020).

[21] Y. Nara and H. Stoecker, Phys. Rev. C **100**, 054902 (2019).

[22] D. Oliinychenko, A. Sorensen, V. Koch, and L. McLerran, Phys. Rev. C **108**, 034908 (2023).

[23] J. Steinheimer, A. Motornenko, A. Sorensen, Y. Nara, V. Koch, and M. Bleicher, Eur. Phys. J. C **82**, 911 (2022).

[24] M. Omana Kuttan, J. Steinheimer, K. Zhou, and H. Stoecker, Phys. Rev. Lett. **131**, 202303 (2023).

[25] A. Li, G.-C. Yong, and Y.-X. Zhang, Phys. Rev. D **107**, 043005 (2023).

[26] Z.-M. Wu and G.-C. Yong, Phys. Rev. C **107**, 034902 (2023).

[27] G.-C. Yong, Phys. Lett. B **848**, 138327 (2024).

[28] L. Adamczyk *et al.* (STAR Collaboration), Phys. Rev. Lett. **112**, 162301 (2014).

[29] L. Adamczyk *et al.* (STAR Collaboration), Phys. Rev. Lett. **120**, 062301 (2018).

[30] H. Stöcker, Nucl. Phys. A **750**, 121 (2005).

[31] Y. Nara, A. Jinno, K. Murase, and A. Ohnishi, Phys. Rev. C **106**, 044902 (2022).

[32] Y. B. Ivanov and A. A. Soldatov, Phys. Rev. C **91**, 024915 (2015).

[33] L. Du, C. Shen, S. Jeon, and C. Gale, Phys. Rev. C **108**, L041901 (2023).

[34] P. Parfenov, Particles **5**, 561 (2022).

[35] M. Mamaev and A. Taranenko, Particles **6**, 622 (2023).

[36] M. Kozhevnikova and Y. B. Ivanov, Phys. Rev. C **109**, 014913 (2024).

[37] J. Steinheimer, J. Auvinen, H. Petersen, M. Bleicher, and H. Stöcker, Phys. Rev. C **89**, 054913 (2014).

[38] S. Chatterjee and P. Bożek, Phys. Rev. Lett. **120**, 192301 (2018).

[39] P. Bożek, Phys. Rev. C **106**, L061901 (2022).

[40] Z.-F. Jiang, S. Cao, X.-Y. Wu, C. B. Yang, and B.-W. Zhang, Phys. Rev. C **105**, 034901 (2022).

[41] M. S. Abdallah *et al.* (STAR Collaboration), Phys. Lett. B **827**, 137003 (2022).

[42] H. Liu *et al.* (E895 Collaboration), Phys. Rev. Lett. **84**, 5488 (2000).

[43] P. Chung *et al.* (E895 Collaboration), Phys. Rev. Lett. **85**, 940 (2000).

[44] D. B. Kaplan and A. E. Nelson, Phys. Lett. B **175**, 57 (1986).

[45] G. E. Brown, C. M. Ko, Z. G. Wu, and L. H. Xia, Phys. Rev. C **43**, 1881 (1991).

[46] T. Waas, N. Kaiser, and W. Weise, Phys. Lett. B **379**, 34 (1996).

[47] J. Schaffner and I. N. Mishustin, Phys. Rev. C **53**, 1416 (1996).

[48] G.-Q. Li, C. M. Ko, and B.-A. Li, Phys. Rev. Lett. **74**, 235 (1995).

[49] S. Pal, C. M. Ko, Z. Lin, and B. Zhang, Phys. Rev. C **62**, 061903(R) (2000).

[50] H. Liu, S. Panitkin, and N. Xu, Phys. Rev. C **59**, 348 (1999).

[51] A. Białas and J. Czyzewski, Phys. Lett. B **222**, 132 (1989).

[52] Z.-W. Lin, Phys. Rev. C **98**, 034908 (2018).

[53] Y. Nara, N. Otuka, A. Ohnishi, K. Niita, and S. Chiba, Phys. Rev. C **61**, 024901 (1999).

[54] Z. Liu, EPJ Web Conf. **296**, 05007 (2024).
[55] H. Sorge, Phys. Rev. C **52**, 3291 (1995).
[56] Z.-W. Lin, C. M. Ko, B.-A. Li, B. Zhang, and S. Pal, Phys. Rev. C **72**, 064901 (2005).
[57] K. Nayak, S. Shi, N. Xu, and Z.-W. Lin, Phys. Rev. C **100**, 054903 (2019).
[58] W. Cassing and E. L. Bratkovskaya, Nucl. Phys. A **831**, 215 (2009).
[59] T. Hirano and Y. Nara, PTEP **2012**, 01A203 (2012).

[60] H. Sorge, H. Stoecker, and W. Greiner, Ann. Phys. **192**, 266 (1989).
[61] S.-W. Lan and S.-S. Shi, Nucl. Sci. Tech. **33**, 21 (2022).
[62] Y. Nara, T. Maruyama, and H. Stoecker, Phys. Rev. C **102**, 024913 (2020).
[63] P. Parfenov *et al.* (MPD Collaboration), Phys. Part. Nucl. **52**, 618 (2021).
[64] C. Zhang, J. Chen, X. Luo, F. Liu, and Y. Nara, Phys. Rev. C **97**, 064913 (2018).